Simultaneous Measurement of Polymerization Kinetics and Stress Development in Radiation-Cured Coatings: A New Experimental Approach and Relationship between the Degree of Conversion and Stress

Andrei A. Stolov, Tao Xie, Jacques Penelle, and Shaw L. Hsu*

Polymer Science and Engineering Department and Materials Research Science and Engineering Center, University of Massachusetts, Amherst, Massachusetts 01003

Received March 6, 2000; Revised Manuscript Received July 11, 2000

ABSTRACT: Stress buildup and polymerization kinetics in UV-cured multifunctional (functionality 4−8) acrylic monomers in coating fabrications have been studied simultaneously using a newly developed combined cantilever deflection method and real-time infrared spectroscopy technique. The macroscopic phenomenon in terms of stress in the film to the molecular architecture in terms of cross-link density has been correlated. Stress buildup was observed to not occur instantaneously after radiation was introduced but rather after a certain time interval. This time interval with respect to onset of polymerization is attributed to the buildup of cross-links, leading to a gel state. Furthermore, it is possible to directly associate stress development with degree of chemical reaction. These experimental observations regarding the gelation point are compared to a number of models presented in the literature. In addition, we have developed a different approach incorporating the probability of finding a relative concentration of reacted or partially reacted monomers relating the stress and degree of conversion of vinyl groups. The predicted stress−conversion relationship based on percolation models is not in good agreement with our experimental data.

Introduction

As polymer coatings are utilized in virtually all products used in society, research in this area ranks among the most important branches of the chemical sciences. Our homes, furniture, and automobiles all employ polymer coatings as protective layers. Firms producing the most advanced optoelectronic devices have a significant interest in development of uniformly thin, yet durable films. Photolithography, packaging of electronic components, labeling of devices, and cladding of high-speed fiber optics which form the backbone of a network all employ thin polymer films. Various medications are coated for controlled speed and ease of delivery. Coating properties of adhesives, composites, and laminates are critical to the performance of engineering materials.

Among the several methods for preparation of polymer coatings, radiation curing is potentially one of the most effective. The advantages of using radiation include the following: (1) environmentally friendly: no organic volatile compounds are employed; (2) high speed: radiation-induced reactions can be extremely efficient and transform liquids to solids within a fraction of a second; (3) spatial resolution: radiation-induced reactions occur only at locations under illumination; (4) ambient temperature operation. The primary use of radiation-cured systems is in film or coating applications. New candidates are being developed in our laboratories that are capable of being cured to form coatings efficiently and of high quality. Our effort is directed at development of new candidates of lower cost, lower irritant to humans, high sensitivity, long shelf life, and environmentally friendly.

* To whom correspondence should be sent.

As in all coating applications, stress development is of concern. When coatings are cured, stress develops as the liquid (solution or dispersion) transforms into an elastic or viscoelastic solid. Since the coating by definition adheres to a substrate, shrinkage can occur only in the thickness direction. The constrained or frustrated volume change in the direction parallel to the substrate leads to an in-plane stress which can lead to defects such as buckling, cracking, curling, and delamination, all of which degrade final coating quality.[1−6] Despite the importance of the problem, few attempts have been made to relate microscopic changes in the molecular structure to stress in radiation-cured coatings.[7] To analyze the factors affecting stress development in thin films, it is crucial to simultaneously measure the structural and stress data from one and the same sample. If two samples are prepared for two separate experiments, slight differences in substrate and film thickness can significantly alter the data. Even environmental humidity may alter the effective film stress.[4,8,9] Thus, only simultaneously obtained stress−polymerization data should be used as a basis for linking micro- and macroscopic changes in radiation-cured coatings. Without a simultaneous measurement of stress and conversion, the determination of the critical degree of conversion for gelation may be in error.

To simultaneously conduct the two measurements, we incorporated the ideal features of two techniques used previously, i.e., miniature cantilever and reflectance infrared spectroscopy. The sensitivity obtained with use of the cantilever deflection method for stress measurement has been demonstrated.[7,10−15] We have used reflectance spectroscopy in many different applications to monitor thin film structure.[16−21] In this current study, we incorporated reflectance infrared spectroscopy to monitor chemical changes in thin films deposited on

10.1021/ma000402r CCC: $19.00
Published on Web 08/23/2000

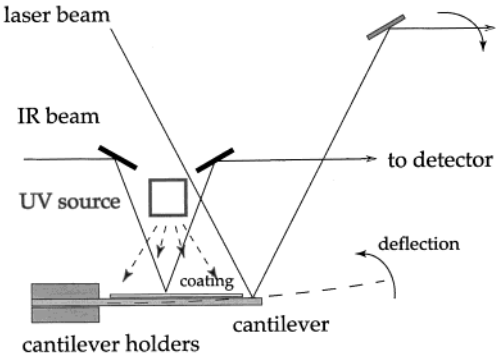

Figure 1. Schematics diagram describing experimental design for simultaneous measurement of stress development and conversion kinetics in coatings.

metallic substrates. The entire experimental setup can be accommodated in the sample chamber of our spectrometer. Ultraviolet radiation can be introduced using liquid light guides. As presented in the Experimental Section, when controlled remotely, this combination provides high-quality spectroscopic data relating chemical changes in the deposited film to the overall deflection of the cantilever in the presence of stress.

For the multifunctional monomers used, it is anticipated that a highly cross-linked system (gel) will develop. The relationship between functionality and gelation point has been derived using a number of different approaches.[22,23] The accuracy of these models for prediction of gelation behavior of our multifunctional acrylates was tested. The stress developed in these coatings was assumed to be related to the volume contraction in formation of the cross-linked structure. The relative concentration of reacted and unreacted monomers is considered as a function of time, dosage, or degree of conversion. An analytical expression was derived and fitted to our experimental data. Our experimental results and analysis are reported here.

Experimental Section

Materials. The monomers and photoinitiator are available commercially and used as received. (Aldrich). The curing behavior of the following monomers have been studied: tripropylene glycol diacrylate ($H_2C{=}CH{-}C(O){-}(OC_3H_6)_3{-}OC(O){-}CH{=}CH_2$, TPGDA), trimethylolpropane triacrylate (($H_2C{=}CH{-}C(O){-}OCH_2)_3C{-}C_2H_5$, TMPTA), and pentaerythritol tetraacrylate ($C(CH_2O{-}C(O){-}CH{=}CH_2)_4$, PETA). The photoinitiator is 2-benzyl-2-(dimethylamino)-4′-morpholinobutyrophenone (Irgacure 369).[24,25] The concentration of the photoinitiator in the formulation was 0.20 mol %. The cantilever deflection setup was validated using a 15% solution of poly(isobutyl methacrylate) (PIBM, $M_w = 130\,000$) in toluene. Both PIBM and toluene were purchased from Aldrich and used as received.

Development of a New Technique. A new apparatus was constructed to measure stress buildup during chemical transformation (see Figure 1). To measure the stress in a coating, a cantilever deflection method is applied.[7,10−15] A coating formulation is applied directly onto the cantilever, the mechanical properties of which are known. One end of the cantilever is clamped; the other is free. Polymerization occurs when the radiation source is turned on. As the relative contraction between the polymer coating and the substrate is different, a stress develops which causes the free end of the cantilever to deflect upward. The changing curvature of the cantilever is measured using the laser beam reflected from the free end. It is possible to accurately measure the cantilever deflection by having a long optical lever arm. Using the following expression, the magnitude of the stress can be calculated:[7,10−15]

$$\sigma_F = \frac{1}{6}\frac{E_S t_S^3}{(1-\nu_S)(t_S + t_F)t_F}\left(\frac{1}{R} - \frac{1}{R_0}\right) \quad (1)$$

where the subscripts F and S denote the film and substrate, respectively; E, ν, and t are the Young's modulus, Poisson's ratio, and thickness, respectively; and R_0 and R are the curvature radii of the cantilever before and during UV curing, respectively. The cantilevers were cut from 0.1 mm thick steel sheets ($E_S = 175$ GPa, $\nu_S = 0.29$[13]). Steel sheets are often used for cantilevers[7,8] since they are relatively inexpensive and have stable elastic properties. The steel sheets were purchased from Small Parts Inc. The cantilevers (5 cm × 0.5 cm) were cut from a sheet 0.6 × 0.3 m. The long axis of the cantilever is parallel to the long axis of the overall sheet. Even though the physical properties of the cantilever is uniform, the steel sheet may exhibit a small degree of anisotropy and slight curvature. Thus, it is important to keep the long axis of the sheet and cantilever to be parallel in all the studies carried out here.

A 3010-EC Dymax UV lamp was used as the UV radiation source. This UV source contains a 100 W, short arc mercury vapor bulb exhibiting radiation mostly in the 320−390 nm region. The UV energy was measured by the IL390B Light Bug radiometer (International Light) and adjusted by changing the source-to-coating distance. The typical radiation intensities used in our experiments were of the order of 10^{-1}−10^2 mW cm^{-2}. Radiation is introduced using liquid guide optics. A remote on/off switch was used.

To follow the chemical changes in the sample, reflection−absorption infrared spectra were registered simultaneously with stress measurements. For this, the cantilever deflection setup was mounted into a Specac external reflection assembly. Reflection−absorption spectroscopy was conveniently carried out using the incidence angle of 30° and film thickness in the range 20−100 μm. It is not necessary to consider the differences between s- and p-polarized IR beams since a considerable number of antinodes exist for the IR standing wave within the films.[17−19]

The entire setup, shown in Figure 1, is accommodated in a Perkin-Elmer system 2000 Fourier transform infrared spectrometer. Typical spectral resolution was 4 cm^{-1}. The time resolution achievable is ∼2 s. The signal-to-noise ratio obtained for this *one-bounce* experiment is quite good and adequate for our analysis. Examples of the spectra obtained before and after UV curing are shown in Figure 2. Bands marked by stars are assignable to monomers and can be used as a measure of the content of the unreacted vinyl groups. The bands at 3106, 3108, and 3107 cm^{-1} belonging to CH_2 stretching vibrations of the vinyl groups of TPGDA, TMPTA, and PETA, respectively, were found to be the most convenient for performing the quantitative analysis. All analyses were based on peak height measured. With the low photoinitiator concentration employed, our spectroscopic data have indicated a uniform degree of conversion through out the film. It is known, however, that degree of conversion or stress can depend on intensity attenuation, photoinitiator concentration, or film thickness. That will be reported separately.

To monitor the stress buildup, we employed a high-speed video camera (Kodak Ektapo HS motion analyzer, model 4540) synchronized with the on−off switch of the UV source. This camera can record the deflection of the laser beam on the screen. The lever arm was about 5 m. A temporal resolution of 30−60 frames per second was found to be sufficient for the system under investigation. All measurements were carried out at 25 °C. Although polymerization of acrylates is not an exothermic process, we have inserted a miniature thermocouple in the film and measured the actual temperature rise to be no more than 2−3 deg. To prevent the chemical reactions being inhibited by oxygen, the experimental chamber was flushed with boiled off nitrogen gas.

Results and Discussion

Validation. To validate our measurement technique, we examined the stress development for a solvent cast

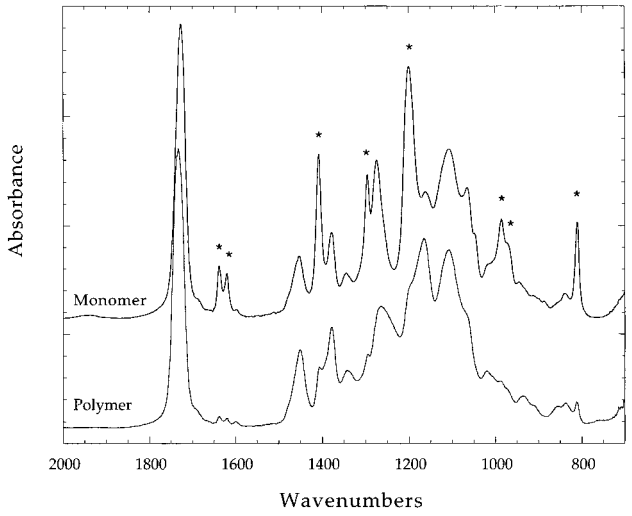

Figure 2. Infrared spectra of TPGDA before (upper trace) and after (lower trace) UV curing. The bands marked by stars represent the features of unreacted vinyl groups.

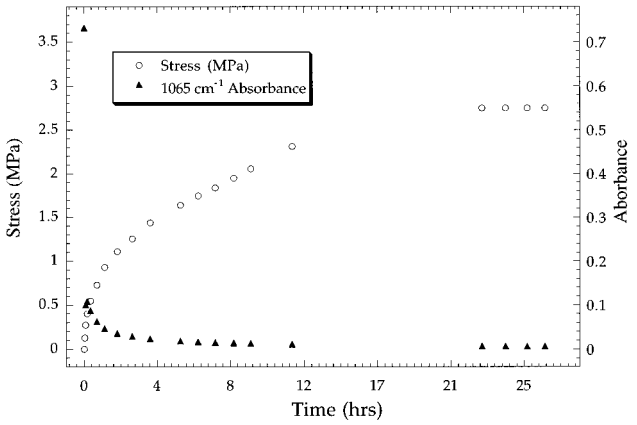

Figure 3. Stress development and solvent evaporation kinetics in a solvent-cast film PIBM/toluene. The content of the solvent was determined based on the intensity of the infrared-active 1065 cm^{-1} band assignable to toluene.

coating of a solution containing 15 wt % of PIBM in toluene. In this case, as shown in Figure 3, stress builds up when the solvent is evaporated. The ultimate stress, σ_F, obtained in our study is 2.7 ± 0.2 MPa at 25 °C. This value is slightly smaller than that found earlier (3.3 ± 0.4 MPa).[7,13] However, in the previous study, σ_F was measured at 21 °C. We investigated the temperature dependence of the stress in PIBM coatings. It was found that the temperature derivative of σ_F equals 0.1 ± 0.01 MPa K^{-1} (Figure 4). Taking this into account, the stress we measure at 21 °C is 3.1 ± 0.2 MPa, which agrees well with previous studies. These results provide the confidence that our experimental setup reliably measures stress values in thin films.

It is also important to investigate the accuracy in use of our spectra to monitor the degree of conversion. It is known that the initial rate of photoinduced polymerization should be proportional to the square root of the absorbed UV intensity.[22,26,27] By varying radiation intensities in the range 0.5−10 mW cm^{-2}, the polymerization rates for the TPGDA−Irgacure 369 system were determined. It was observed that the above-mentioned relationship indeed holds, confirming the reliability of our measurements and indicating that the theory of photoinduced polymerization is valid for our system.

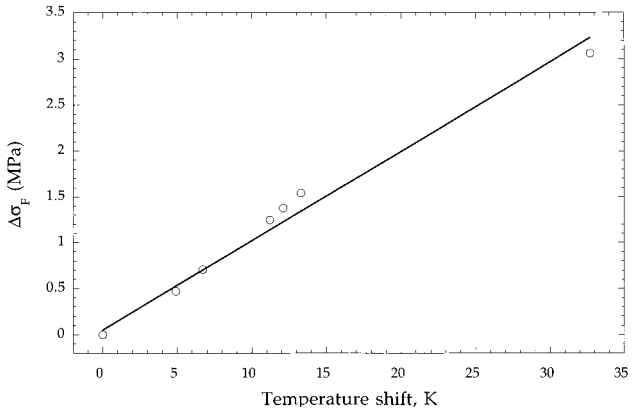

Figure 4. Temperature dependence of internal stress in PIBM solvent cast film on a steel surface. The origin of the plot corresponds to a temperature value of 22 °C.

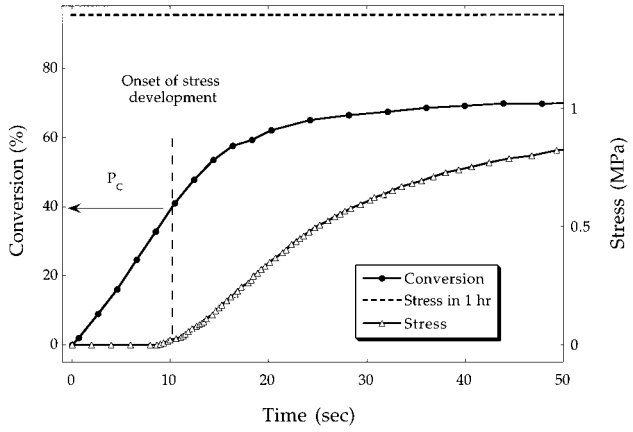

Figure 5. Stress buildup and polymerization kinetics measured for a TPGDA coating (0.2 mol % of Irgacure 369). The dashed line shows the stress magnitude 1 h after start of the experiment. The coating thickness is 73 μm, and the radiation intensity is 0.19 mW cm^{-2}.

Stress/Conversion Measurement. Typical data obtained for stress buildup upon exposure of TPGDA to ultraviolet radiation are shown in Figure 5. It is clear that stress does not develop until approximately 8−9 s after radiation is turned on. The onset of stress buildup corresponds approximately to 35−43% of the conversion of TPGDA vinyl groups. For TMPTA and PETA these critical values, P_c's, are 21−25 and 14−18%, respectively. The functional forms of the degree of conversion and stress buildup have very similar time dependence. However, the degree of conversion nearly reaches the plateau at 30−40 s while, in contrast, the stress continues to increase noticeably with exposure times longer than 40 s. Figure 5 presents only the initial portion of the polymerization and stress buildup process. Typically, the samples were exposed to UV radiation for 800 s, and then radiation was turned off. Stress and conversion data for TMPTA are plotted in Figure 6. It can be seen that even after the UV source is turned off, polymerization continues, causing an additional increase in stress. The "dark" polymerization has been found previously for multifunctional acrylates in both liquid and solid states.[27−29] The solid-state polymerization was shown to be due to radicals trapped in rigid domains of the polymers.[29,30] These radicals may be fragments of the photoinitiator molecules or the unreacted end groups of the monomers. The lifetime of the radicals depends on molecular mobility, which abruptly drops with degree of cross-linking. The residual polym-

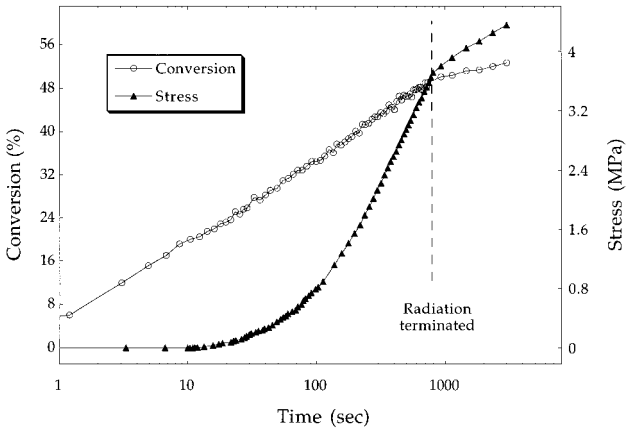

Figure 6. Stress buildup and polymerization kinetics measured for a TMPTA coating (0.2 mol % of Irgacure 369). The coating thickness is 53 μm, and the radiation intensity is 0.29 mW cm^{-2}. The dashed line corresponds to the time when the UV source was turned off.

erization may take a long time, resulting in a significant increase of internal stress. Hence, there is no possibility of measuring the "ultimate" stress of the UV-cured coatings. One should keep in mind that the maximal stress determined experimentally strongly depends on the time at which it is determined.

This 8−10 s delay between stress buildup and introduction of radiation is attributed to the fact that the liquidlike monomer does not initially carry any stress. Stress buildup is assumed to be associated with the film solidification process. In this case, because of the multifunctionality of the acrylates used, the onset of stress buildup is due to gelation. In other systems if the molecular weight is sufficiently high, a glass state may form.[31,32] Several aspects of our system deserve detailed examination. First, it is important to find the critical point of conversion when a gel state is formed. For this state, the glass transition temperature must be very low. Second, it is important to understand the functional form relating the degree of conversion to stress buildup as a function of time. Third, obviously monomer functionality plays a very important role. There is, however, no critical test to reveal the quantitative dependence in radiation curable systems. Each of the abovementioned aspects are analyzed in this report.

A number of theories have been developed to characterize the gelation point. Following Carothers' consideration,[22] the critical degree of conversion at gel point, P_c, is strictly dependent on the functionality of the system

$$P_c = 2/f_{av} \tag{2}$$

where f_{av} is the average functionality of the systems. For TPGDA, TMPTA, and PETA the f_{av} values are 4, 6, and 8, respectively. The obtained magnitudes of P_c are listed in Table 1. It can be seen that both experimental (as determined from the onset of stress build-up) and Carothers' P_c values tend to decrease with monomer functionality. However, the predicted values are systematically higher than those obtained experimentally. This is consistent with previous observations that the Carothers theory often overestimates P_c values.[22,23] The critical degree of cross-linking found in this study for TMPTA (21−25%) is lower than the data reported previously (∼35%).[7] Because of the simultaneous measurement of stress buildup and cross-linking density employed in our study, experimental variations such as difference in environmental humidity, film thickness, radiation intensity, and dosage are eliminated.

Subsequently, Flory[23] and Stockmayer[33] developed a statistical approach to characterize gelation behavior of multifunctional polymers. In their treatments, each monomer unit is supposed to form any (odd or even) number of bonds with other monomer units. In our systems, only even number of bonds can be formed by each molecule. Thus, an extension of the Flory theory becomes necessary.

At any particular time, we have a system containing unreacted, partially reacted, and completely reacted monomers. Let us define P_n as the probability of n vinyl groups reacted in a sample molecule. For a monomer with a maximal functionality f_{max}, such probability equals

$$P_n = C_m^n P^n (1 - P)^{m-n} \tag{3}$$

where P is the vinyl group conversion, $m = f_{max}/2$, and C_m^n are binomial distribution coefficients. Equation 3 assumes equal reactivity of all vinyl groups of the monomers. Following Flory, we define the branching coefficient α as the probability of the structure shown below:

$$M_{>1}-M_1-M_1-...-M_1-M_{>1} \tag{4}$$

where M_1 and $M_{>1}$ are the monomers with one and more reacted vinyl groups, respectively. On the basis of this definition, the branching coefficient can be calculated as

$$\alpha = (\sum_{n=2}^{m} P_n)\sum_{j=0}^{\infty} P_1^{\,j} = (\sum_{n=2}^{m} P_n)/(1 - P_1) \tag{5}$$

The average functionality of the ends, f_{av}^{ends}, of the structure shown by eq 4 in question is

$$f_{av}^{ends} = (\sum_{n=2}^{m} 2nP_n)/\sum_{n=2}^{m} P_n \tag{6}$$

According to the Flory approach, the gelation of the system occurs at

$$\alpha = 1/(f_{av}^{ends} - 1) \tag{7}$$

Substituting eqs 3−6 into eq 7, the conversion of vinyl groups at the gel point may be calculated. The calculated values of P_c are given in Table 1. A quantitative agreement is observed between the experimental data and predictions of this extended Flory theory.

The gelation point can also be treated using the percolation theory.[34] Each molecule may be modeled by a site, the chemical links being the bonds between sites. Depending on the maximal number of bonds emanating from each site (f_{max}), one can assume an appropriate percolation model for each monomer. However, functionality is not the only factor determining the percolation model. For example, for $f_{max} = 6$ one can assume the Bethe lattice, triangular bond lattice, and 3D cubic lattice models, depending on the structure of the gel which is usually unknown. Predictions of some percola-

Table 1. Experimental and Theoretical Magnitudes of P_c (%) for Multifunctional Acrylates

		gelation points (%)							
			molecular theories		percolation theories				
monomer	f_{max}	expt	Carothers	extended Flory	Bethe lattice	square bond lattice	triangular bond lattice	simple cubic lattice	4D cubic lattice
TPGDA	4	35−43	50	41.4	33	50			
TMPTA	6	21−25	33	26.8	20		34.7	24.9	
PETA	8	14−18	25	20.0	14.3				16.7

tion models[35] are given in Table 1. As can be seen, the Bethe lattice and the cubic lattice models produce a somewhat accurate estimate of the observed gelation points.

Our second objective is to deduce a functional relationship between degree of conversion and stress buildup for our systems. Upon curing, the coating tends to shrink in all three dimensions, including that parallel to the substrate. As one would expect that the coating adheres to the substrate, a nonslip boundary condition may be assumed. A small change in the number of converted vinyl groups, dP, causes film shrinkage. Since the substrate tends to keep the area of the coating stable, the actual strain, ϵ, is almost zero. This situation can be modeled equivalent to a two-step process: (1) shrinkage of the film without a substrate ($d\epsilon < 0$, $d\sigma_F = 0$) and (2) stretching the film toward its initial size so that $d\epsilon > 0$. The incremental change in stress is

$$d\sigma_F = \frac{E_F}{1 - \nu_F} d\epsilon \tag{8}$$

In the above expression, E_F is the Young's modulus and ν_F the Poison's ratio of the film. These two values are dependent on degree of conversion. There is no straightforward way to express E_F, ν_F, and ϵ as functions of P, necessitating the use of various assumptions. First, it seems reasonable to assume that each chemical reaction of a vinyl group causes a similar decrease in volume. Thus, the change in the overall strain is proportional to the conversion

$$d\epsilon = \gamma\, dP \tag{9}$$

where γ is a constant. Currently a detailed theory does not exist and needs to be developed. For the purpose of a qualitative comparison, we use the expression relating stress buildup to the number of cross-links as in the rubber elasticity theory.[36] Then the overall sample modulus is proportional to the number of cross-links formed

$$E_F = N_0 RT\left(\frac{\bar{r}_0^{\,2}}{\bar{r}_f^{\,2}}\right) \tag{10}$$

where N_0 is the number of cross-links per unit volume, T is temperature, R is gas constant, and $(\bar{r}_0^{\,2}/\bar{r}_f^{\,2})$ is the front factor. The increase of E_F during the experiment is primarily due to the change of N_0. In addition, the expression for E_F must satisfy the initial condition $E_F(P_c) = 0$. Thus, modifying eq 10, one obtains

$$E_F \sim N_0(P) - N_0(P_c) \tag{11}$$

The relationship between N_0 and P can be deduced on the basis of simple probability considerations. A molecule with n vinyl groups reacted forms $(n - 1)$ cross-link units. Taking into account the probabilities of the species with n groups reacted (eq 3), one obtains

$$N_0 \sim \sum_{n=2}^{m} (n-1)P_n \tag{12}$$

It is generally accepted that $\nu_F \approx 0.5$ for rubbers and $\nu_F < 0.5$ for most solids.[36,37] Unfortunately, it seems virtually impossible to predict the dependence of ν_F on P. It should be noted, however, that the magnitude of $d\sigma_F$ in eq 8 is insignificantly affected by changes of ν_F between 0.5 and 0.3. Thus, it seems reasonable to neglect the dependence of ν_F on P. Substituting eqs 9, 11, and 12 into eq 8 and carrying out the integration from P_c to P, one obtains

$$\sigma_F = B_4[P^3 - 3PP_c^{\,2} - 2P_c^{\,3}] \quad (\text{for } f_{max} = 4) \tag{13}$$

$$\sigma_F = B_6[P^3(4 - P) + 4PP_c^{\,2}(P_c - 3) + P_c^{\,3}(8 - 3P_c)] \quad (\text{for } f_{max} = 6) \tag{14}$$

$$\sigma_F = B_8[P^3(2 - P + 0.2P^2) - PP_c^{\,2}(6 - 4P_c + P_c^{\,2}) + P_c^{\,3}(4 - 3P_c + 0.8P_c^{\,2})] \quad (\text{for } f_{max} = 8) \tag{15}$$

where B's are constants. Experimental values of stress buildup in the TPGDA, TMPTA, and PETA coatings and the calculated values based on eqs 13−15 are superposed in Figures 7−9. The multiplier B_n was adjusted so that the calculation reproduces the experimental σ_F at 3200−3600 s. It can be seen that eqs 13−15 reproduce the functional form of the $\sigma_F = f(t)$ dependence fairly well, especially at short ($10 < t < 30$ s) and long times

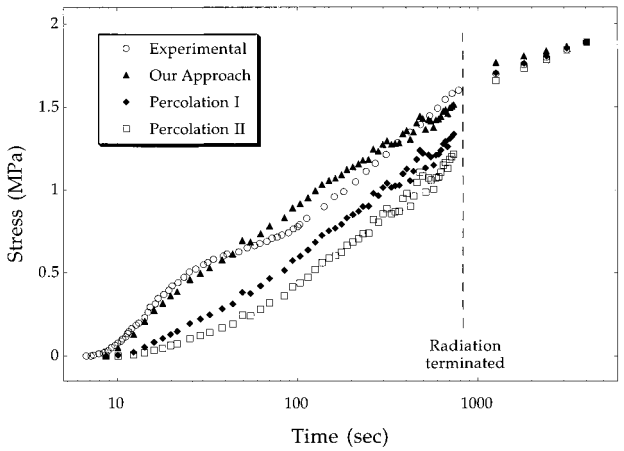

Figure 7. Experimental and theoretical stress−time dependencies for a TPGDA coating (0.2 mol % of Irgacure 369, the coating thickness is 72 μm, and the radiation intensity is 0.18 mW cm^{-2}). The dashed line corresponds to the time when the UV source was turned off. The theoretical curves are the results of fitting the experimental data by eq 13 (our approach) and by eq 17 with $\beta = {}^8/_3$ (percolation I[39]) and $\beta = 3.6$ (percolation II[40]).

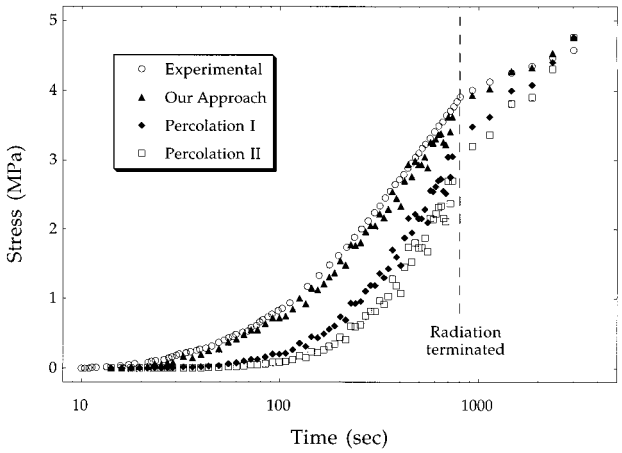

Figure 8. Experimental and theoretical stress−time dependencies for a TMPTA coating (0.2 mol % of Irgacure 369). The coating thickness is 53 μm, and the radiation intensity is 0.29 mW cm^{-2}. The dashed line corresponds to the time when the UV source was turned off. The theoretical curves are the results of fitting the experimental data by eq 14 (our approach) and by eq 17 with $\beta = {}^{8}/_{3}$ (percolation I[39]) and $\beta = 3.6$ (percolation II[40]).

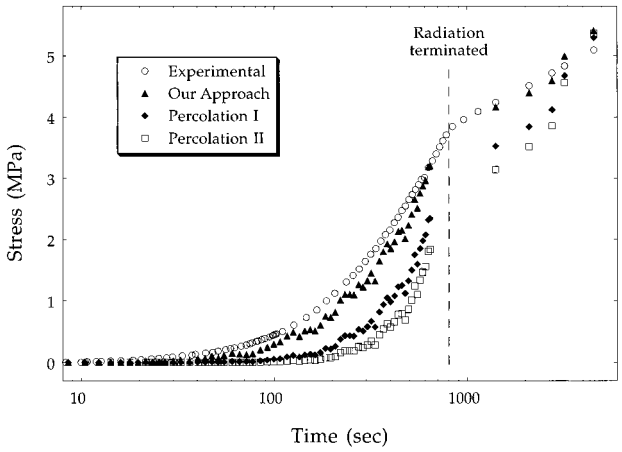

Figure 9. Experimental and theoretical stress−time dependencies for a PETA coating (0.2 mol % of Irgacure 369). The coating thickness is 83 μm, and the radiation intensity is 0.15 mW cm^{-2}. The dashed line corresponds to the time when the UV source was turned off. The theoretical curves are the results of fitting the experimental data by eq 15 (our approach) and by eq 17 with $\beta = {}^{8}/_{3}$ (percolation I[39]) and $\beta = 3.6$ (percolation II[40]).

($t > 400$ s), confirming that stress in the acrylate coating is mainly due to cross-link formation.

Our experimental data present the opportunity to employ percolation models which has generated significant interest in polymer systems.[34] Such models have found applications ranging from electronic conductivity to polyurethane foams.[38−41] Perhaps applications closest to our interest are those dealing with curing behavior of thermosets[39,42,43] and filler networks.[40] In all cases, the percolation model yields an expression for Young's modulus on $(P - P_c)$ as

$$E_F = (P - P_c)^{\beta} \tag{16}$$

where β is a constant, which may differ depending on the model. According to the model of refs 39, 42, and 43, $\beta = {}^{8}/_{3}$, while according to another model $\beta = 3.6$.[40] Applying the integration as in eq 8, one obtains

$$\sigma_F = B_{perc}(P - P_c)^{\beta+1} \tag{17}$$

where B_{perc} is another adjustable constant. Figures 7−9 present the result of application of eq 17. As above, we adjusted the multiplier B_{perc} so that the calculation reproduces the experimental σ_F at 3200−3600 s. It can be seen in Figures 7−9 that both percolation models do not reproduce the experimental data as satisfactorily as eqs 13−15.

Conclusions

The experimental technique combining real-time spectroscopy and a miniature cantilever has been demonstrated to be capable of measuring stress buildup in coatings. The sensitivity of the stress measured is extremely high. By using the reflectance technique, it is possible to obtain high-quality infrared spectra, thus providing information regarding chemical transformation within the coating with accuracy. This technique has been applied to radiation-induced polymerization. The data obtained provide the critical degree of polymerization for gelation to form. In fact, our analysis establishes that gelation necessarily is the mechanism responsible for occurrence of stress buildup in thin coatings. With the data obtained, it is possible to evaluate the accuracy of various models for prediction of the critical degree of conversion. Flory's theory yields values much closer than Carothers' and those based on percolation. From statistics locating various monomers as a function of time, it is also possible to predict stress buildup as a function of conversion for acrylates with functionality 4−8. The effects of substrate anisotropy and film thickness on stress buildup shall be reported in the near future.

Acknowledgment. The authors acknowledge the National Environmental Technology for Waste Prevention Institute for providing support for this study.

References and Notes

(1) Kloosterboer, J. G. *Adv. Polym. Sci.* **1988**, *84*, 1.
(2) Hnojewyj, O.; Murdock, M. S.; Dunker, S. M. In NEPCON, 1992; p 909.
(3) Croll, S. G. *J. Coat. Technol.* **1980**, *8*, 143.
(4) Sato, K. *Prog. Org. Coat.* **1980**, *8*, 143.
(5) Scherer, G. W. *J. Non-Cryst. Solids* **1992**, *148*, 363.
(6) Oosterbroek, M.; Lammers, R. J.; van der Ven, J. J.; Perera, D. Y. *J. Coat. Technol.* **1991**, *66*, 1267.
(7) Payne, J. A.; Francis, L. F.; McCormick, A. V. *J. Appl. Polym. Sci.* **1997**, *66*, 1267−1277.
(8) Negele, O.; Funke, W. *Prog. Org. Coat.* **1996**, *28*, 285−289.
(9) Payne, J. A.; McCormick, A. V.; Francis, L. F. *J. Appl. Polym. Sci.* **1999**, *73*, 553−561.
(10) Ree, M.; Chu, C.-W.; Coldberg, M. J. *J. Appl. Phys.* **1994**, *75*, 1410−1419.
(11) Ree, M.; Shin, T. J.; Park, Y.-H.; Kim, S. I.; Woo, S. H.; Cho, C. K.; Park, C. E. *J. Polym. Sci., Polym. Phys.* **1998**, *36*, 1261−1273.
(12) Perera, D. Y.; Vanden Eynde, D. *J. Coat. Technol.* **1981**, *53*, 40−45.
(13) Croll, S. G. *J. Coat. Technol.* **1978**, *50*, 33−38.
(14) Coburn, J. C.; Pottiger, M. T.; Noe, S. C.; Senturia, S. D. *J. Polym. Sci., Polym. Phys.* **1994**, *32*, 1271−1283.
(15) Perry, A. J.; Albert Sue, J.; Martin, P. J. *Surf. Coat. Technol.* **1996**, *81*, 17−28.
(16) Meuse, C. W.; Tao, H.-J.; Hsu, S. L.; MacKnight, W. J. *Polym. Prepr. (Am. Chem. Soc., Div. Polym. Chem.)* **1993**, *34*, 266−267.
(17) Ren, Y.; Meuse, C. W.; Hsu, S. L.; Stidham, H. D. *J. Phys. Chem.* **1994**, *98*, 8424.
(18) Ren, Y.; Shoichet, M. S.; McCarthy, T. J.; Stidham, H. D.; Hsu, S. L. *Macromolecules* **1995**, *28*, 358.

(19) Ren, Y. *Spectroscopic Investigations of Polymers and Polymer Surfaces/Interfaces*; University of Massachusetts: Amherst, MA, 1995.
(20) Riou, S. A.; Hsu, S. L.; Stidham, H. D. *J. Polym. Sci., Polym. Phys.* **1997**, *35*, 2843−2855.
(21) Su, Z. H.; Wu, D. C.; Hsu, S. L.; McCarthy, T. J. *Abstr. Pap. Am. Chem. Soc.* **1997**, *213*, 487-Poly, Part 2.
(22) Odian, G. *Principles of Polymerization*; Wiley: New York, 1991.
(23) Flory, P. J. *Principles of Polymer Chemistry*; Cornell University Press: Ithaca, NY, 1953.
(24) Desobry, V.; Dietliker, K.; Husler, R.; Misev, L.; Rembold, M.; Rutsch, W. *A Novel Photoinitiator for Modern Technology*; American Chemical Society: Washington, DC, 1989; Vol. 60, pp 26−30.
(25) Desobry, V.; Dietliker, K.; Husler, R.; Misev, L.; Rembold, M.; Rist, G.; Rutsch, W. *A Novel Photoinitiator for Modern Technology*; Hoyle, C. E., Kinstle, J. F., Eds.; American Chemical Society: Washngton, DC, 1990; Vol. 417, pp 92−105.
(26) Tryson, G. R.; Schultz, A. R. *J. Polym. Sci., Polym. Phys.* **1979**, *17*, 2059−2075.
(27) Decker, C. *Prog. Polym. Sci.* **1996**, *21*, 593−650.
(28) Decker, C.; Moussa, K. *Makromol. Chem.* **1988**, *189*, 2381−2394.
(29) Selli, E.; Bellobono, I. R.; Oliva, C. *Macromol. Chem. Phys.* **1994**, *195*, 661−669.
(30) Selli, E.; Oliva, C. *Macromol. Chem. Phys.* **1996**, *197*, 497−507.
(31) Cook, W. D. *Polymer* **1992**, *33*, 2152−2161.
(32) Cook, W. D. *J. Polym. Sci., Polym. Chem.* **1993**, *31*, 1053−1067.
(33) Stockmayer, W. H. *J. Chem. Phys.* **1943**, *11*, 45−55.
(34) Grimmet, G. *Percolation*; Springer-Verlag: New York, 1980.
(35) Stauffer, D. *Introduction to Percolation Theory*; Taylor & Francis: London, 1985.
(36) Aklonis, J. J.; MacKnight, W. J. *Introduction to Polymer Viscoelasticity*, 2nd ed.; John Wiley and Sons: New York, 1983.
(37) Timoshenko, S. *Theory of Elasticity*; McGraw-Hill Book Company, Inc.: New York, 1934.
(38) Coniglio, A. *Phys. Rev. Lett.* **1981**, *46*, 250−253.
(39) Adolf, D. B.; Martin, J. E.; Chambers, R. S.; Burchett, S. N. *J. Mater. Res.* **1998**, *13*, 530−550.
(40) Kluppel, M.; Schuster, R. H.; Heinrich, G. *Rubber Chem. Technol.* **1997**, *70*, 243−255.
(41) Yontz, D. J.; Hsu, S. L.; Lidy, W. A.; Gier, D. R.; Mazor, M. H. *J. Polym. Sci., Polym. Phys.* **1998**, *36*, 3065−3077.
(42) Adolf, D. B.; Martin, J. E. *J. Compos. Mater.* **1996**, *30*, 13−34.
(43) Adolf, D. B.; Chambers, R. *Polymer* **1997**, *38*, 5481−5490.

MA000402R